



Instrument Science Report NICMOS 2009-001

New Bad Pixel Mask Reference Files for the Post-NCS Era

Elizabeth A. Barker and Tomas Dahlen
June 08, 2009

ABSTRACT

The last determined bad pixel masks for the three NICMOS cameras were made in September 2002. Those masks were created using data from calibration programs following the installation of the NCS and are therefore based on the relatively limited data set available at the time. Since then, the NICMOS calibration monitoring programs have regularly obtained calibration images of both flat-fields and darks, images used to create the mask reference files. With numerous images taken during a long base-line (2002-2008), this data set allows us to create high signal-to-noise reference files, as well as investigate any temporal dependence of the mask files. In this ISR we describe the creation of new mask files based on this extended data set and compare the new masks with the previous versions. The new masks created contain a higher number of bad pixels compared to the old versions, while the number of pixels thought to be affected by “grot” is lower.

Introduction

The NICMOS detectors are regularly calibrated through the use of flat-field and dark reference images. Studying these reference images provides a tool to understand the behavior of individual pixels, as well as any evolution with time. The NICMOS data quality (DQ) extension of calibrated images (*_ima.fits or *_cal.fits) contains specific information regarding problematic pixels, which should be considered for exclusion when science images are combined or dithered. This DQ extension identifies

several different types of problems that may affect pixels, including both static flag values, which do not depend on the observation, and dynamic flag values, which are set based on the observation or the subsequent calibration. The static flags for “bad” pixels and “grot” pixels are identified with separate DQ values (DQ=32 and DQ=16, respectively). Each NICMOS camera has two unique static masks, one for use with pre-NCS data and one for use with post-NCS data. The relevant mask for each observation is identified in the header keyword MASKFILE of the science images and has the *_msk.fits extension.

A proper removal of bad pixels from NICMOS images is important for securing the data quality of reduced images. Initial bad pixel masks were created during Systems Level Thermal Vacuum ground testing prior to the installation of NICMOS on HST. Newer bad pixel masks for pre-NCS data were created in 2002, based on in-flight data taken in 1997-8 (Sosey 2002, NICMOS ISR 2002-001), however these masks were not delivered to the CDBS database until 2009.

In 2002, the NICMOS Cooling System (NCS) was installed on HST and connected to NICMOS during Service Mission 3b. The NCS consists of a cryocooler and re-enabled NICMOS for science observations, but at a higher nominal operating temperature. After the installation of the NCS, masks for post-NCS data were created in September 2002 using in-flight data.

The dark reference frames measure the accumulation of signal due to dark current, per pixel, during observations. Studying the variation of dark current pixel-by-pixel is necessary to understand the inherent variations across the detectors. Since the dark images measure the signal accumulated without any external illumination, they are an excellent device to detect defective pixels with deviant behavior. Hot pixels have excessive charge and cold have little or no charge, even with significant exposure times. To study the bad pixels of the detectors, we have analyzed dark reference files taken during the post-NCS era of 2002-2008.

An additional type of bad pixel exists on the NICMOS detectors, often referred to as *grot*-affected pixels. As a result of the deformation of the NICMOS instrument, we believe paint flecks (ranging in size from a fraction of a pixel to a few pixels) were deposited on the detectors of all three cameras. They are apparent in all images where an external source of illumination is used. Grot-affected pixels appear as pixels with lower signal response compared to neighboring pixels. Since flat-field images have a high and uniform illumination, they are well suited for detecting grot pixels. Thus, we have analyzed the flat-field calibration images to study the behavior of grot pixels since SM3b and have determined a new set of grot pixels appropriate for post-NCS observations.

Since these data have been taken during a large part of the post-NCS era, investigating changes of the bad pixels with time is now also possible.

Data and Reduction

In order to determine hot and cold pixels, we use data taken during the dark monitoring programs 2002-2008 (programs 9321, 9636, 9993, 10380, 10723, 11057, 11318) together with data taken during the extended darks program (11330), which started early 2008. The number of exposures for each different SAMP_SEQUENCE per NICMOS camera is shown in Table 1. We use SPARS64 with NSAMP of 20, 24 and 26, giving exposure times of over 1000s. All used the BLANK filter position, as is typical for dark observations.

SAMP_SEQ	NSAMP	Exp Time	NIC1	NIC2	NIC3
SPARS64	20	1088s	290	290	290
SPARS64	24	1344s	477	478	478
SPARS64	26	1472s	30	30	30
Total Images			797	798	798

Table 1: Number of dark images for the read out modes for the three NICMOS detectors.

The grot-affected pixels were analyzed by examining flat-field data from 2002 to 2008 (programs 8974, 8985, 9326, 9327, 9640, 9996, 10379, 10728, 11016, 11059, 11321) with the F160W filter, which is well-sampled including more than 100 individual images per camera.

Bad (DQ=32) Pixels

In order to identify both hot and cold (collectively “bad”) pixels, we examine long exposure dark images with exposure times greater than 1000s (see Table 1). Long exposures make the identification of both types of bad pixels easier to identify, when compared to neighboring pixels and expected values for dark current. “Hot” pixels are defined to be those that exhibit excessive charge when compared to surrounding pixels. “Cold” pixels are those that have extremely low or near zero response or dark current (also known as “dead” pixels).

For consistency and continuity, we utilize the same method of identifying bad pixels as that given in NICMOS ISR 2002-001 (Sosey 2002). Specifically:

1. Each dark reference image is CR cleaned.
2. A composite median dark image is created from the CR-cleaned darks.
3. A smoothed composite image is created from the composite median dark image.
4. The smoothed composite is subtracted from the composite median dark image.
5. The subtracted composite image is rescaled to units of its RMS.
6. Bad pixels are identified in the subtracted composite image as those pixels outside of 5σ .

Time Dependence of Bad Pixels

Since we are not only interested in knowing if any new pixels have changed into bad pixels, we also look for changes in time. This is now possible, since we have nearly-continuous dark calibration images between 2002 and 2008 (post-NCS era). Table 2 shows the number of bad pixels, per camera, found in the old post-NCS masks from 2002, as well as the number of additional bad pixels found each year compared to the old mask.

	NIC 1	NIC 2	NIC 3
Old DQ=32	193 (0.29%)	656 (1.0%)	446 (0.68%)
2002	46	17	16
2003	49	21	21
2004	70	28	28
2005	69	24	30
2006	70	24	29
2007	66	29	34
2008	70	31	36
All new	88 (+0.13%)	40 (+0.06%)	42 (+0.06%)

Table 2: Number of *additional* bad pixels per year per camera. “Old DQ=32” represents the number pixels in the 2002 post-NCS bad pixel masks. “All new” represents the number of completely new bad pixels over the whole time range 2002-2008.

The number of bad pixels in the old post-NCS bad pixel masks from 2002 are listed for each camera. For each year in the post-NCS era, we have tabulated the number of *additional* bad pixels found in this investigation. On the last line, we list the total number of different pixels that are flagged as bad during at least one year. This can also be seen in Figure 1.

Note that all “new” bad pixels we find are hot and there are no new “dead” pixels found compared to the 2002 post-NCS bad pixel masks. There could still be new cold pixels

that are not selected by the above criteria, however such pixels will be selected as grot pixels in the next step if the decrease in response of the pixel is significant.

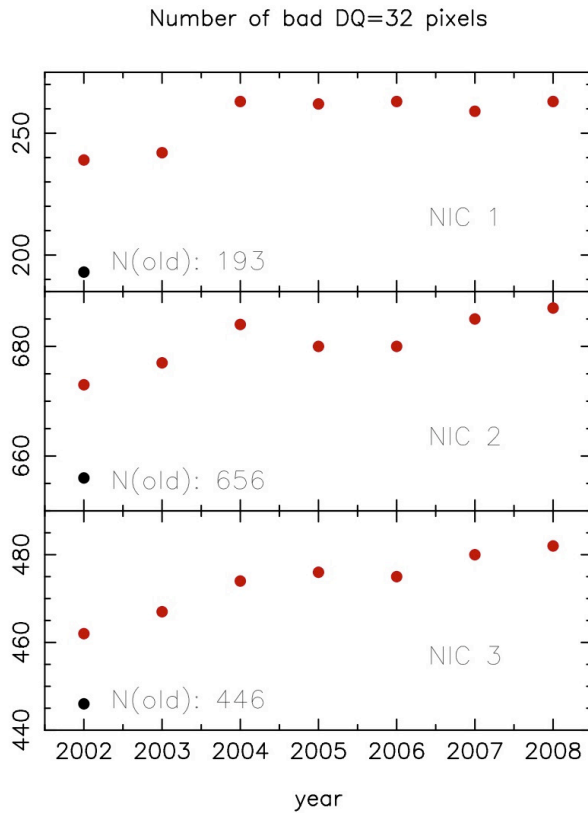


Figure 1: Number of new bad pixels by year and camera. The lower black dot for 2002 represents the old mask. The remaining dots show the total number of bad pixels per year, including all old pixels and additional new pixels for each year.

Figure 1 shows the number of bad pixels in the previous bad pixel masks, for each camera, as a black dot in 2002. Shown in red dots are the total number of bad pixels per year in the post-NCS bad pixel masks found in this investigation. All of these bad pixels, both hot and cold, are flagged with DQ=32 in the *_msk.fits files, as well as in the calibrated *_ima.fits and *_cal.fits files.

As a primary approach, we create new bad pixel masks by adding all new pixels (bottom row of Table 2) to the existing masks. However, since we know that the number of bad pixels is changing with time, it is worthwhile to study how many pixels can be “saved” as scientifically useful pixels by having multiple bad pixel masks, one per year, for instance. If the number is significant, such an approach may be justifiable.

To examine the number of pixels that can be returned to scientific use during at least one year by creating a bad pixel mask per year, we plot in Figure 2 the RMS of all pixels that are selected as hot ($\text{RMS} > 5\sigma$) during at least one of the seven years. Good pixels that suddenly turn bad are characterized by initially have a low RMS ($<1\sigma$), where after they turn bad and show $\text{RMS} > 5\sigma$. Similarly, there are pixels that start out bad ($\text{RMS} > 5\sigma$), but with time drop in RMS. If the number of these pixels had been high, then the multiple mask approach would be justifiable. However, studying Figure 2 shows that only a handful of pixels have low RMS ($\sim 1\sigma$) during part of the whole period. This small number of pixels does not justify having multiple masks. Instead, we create new bad pixel masks including all pixels that have $\text{RMS} > 5\sigma$ during at least one epoch.

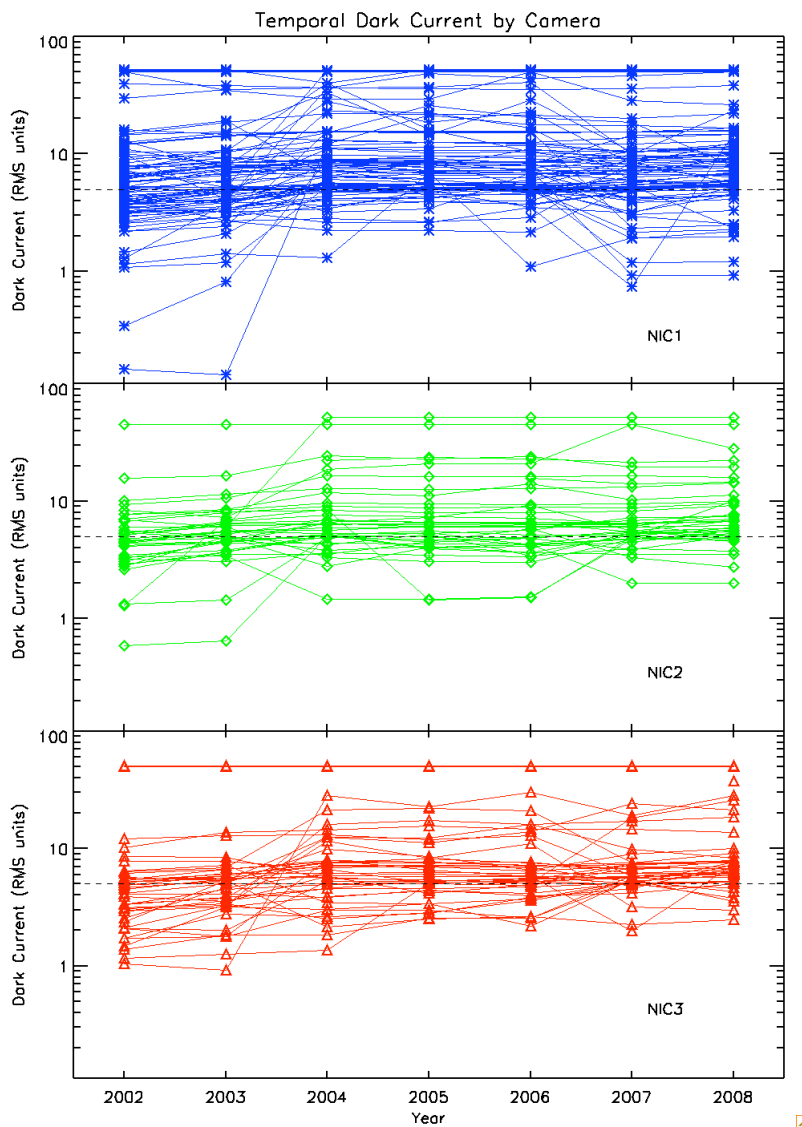


Figure 2: The dark current of the darks (in RMS units) versus year, by camera, for all additional bad pixels found in this investigation. The dotted line represents the 5σ cutoff.

Figure 3 shows the old bad pixel mask (top row) and the new bad pixel mask (bottom row) for each camera.

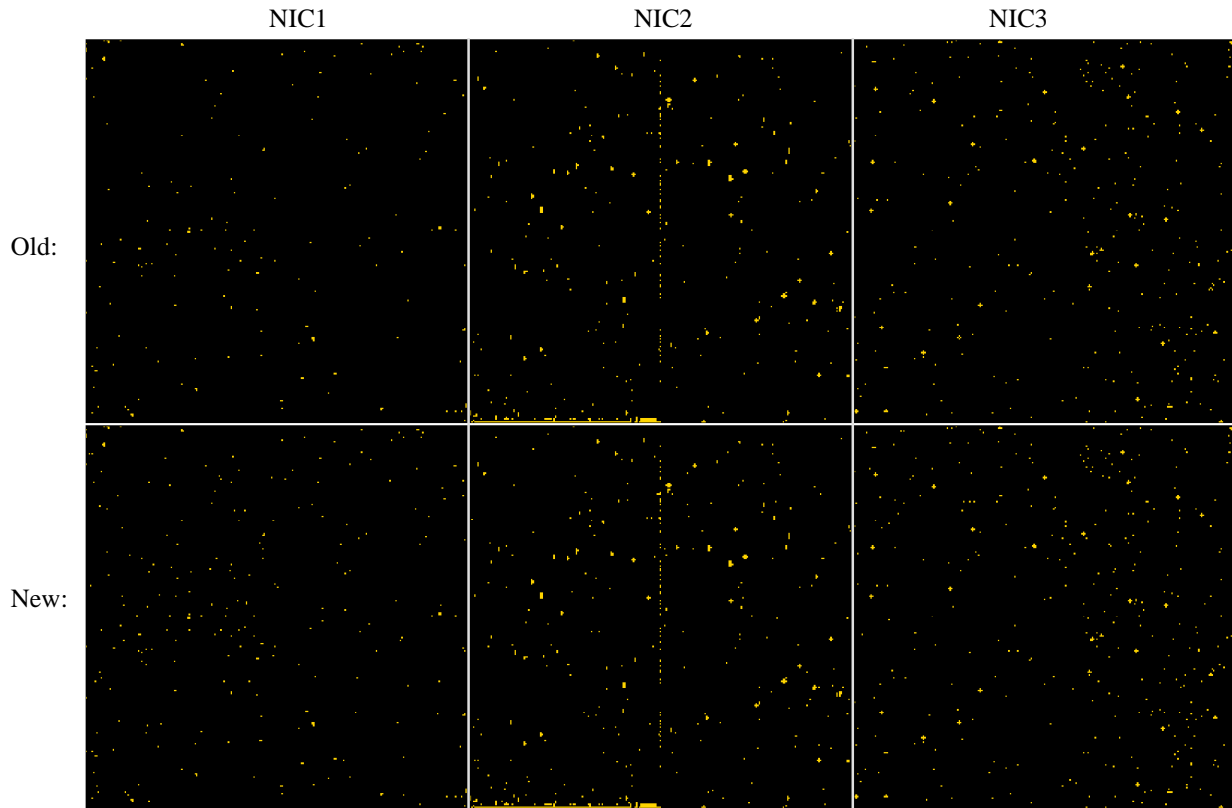


Figure 3: The old (top row) and new (bottom row) bad pixel masks (DQ=32 only) for each camera.

Grot (DQ=16) Pixels

Grot is believed to be flecks of anti-reflective paint deposited on the detectors when the expansion of the solid nitrogen caused the optical baffles to scrape against each other (see NICMOS ISR 99-008 for a complete discussion). Grot produces small areas of reduced sensitivity, ranging in size from $25\mu\text{m}$ to $100\mu\text{m}$. Since NICMOS pixels are $40\mu\text{m}$ on each side, grot can affect less than one pixel up to several pixels by a single fleck. The largest example of a single grot region is called the “battleship” feature in NIC1 (see Figure 4), which affects approximately 35 pixels.

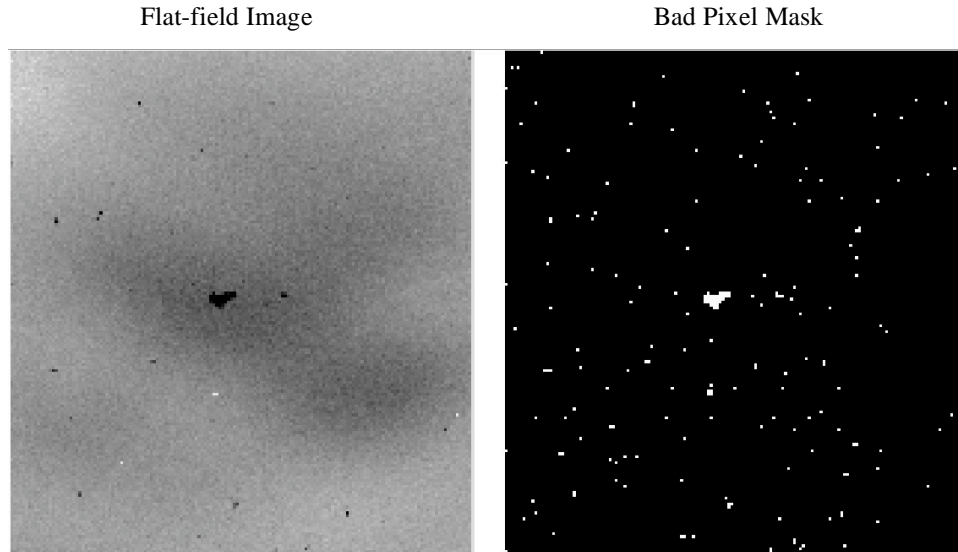


Figure 4: The largest grot feature, known as the "battleship", can be seen in NIC1.

Since grot consists of a physical substance on the detectors, it affects the incoming light landing on the detectors. Since flat-field exposures are uniformly illuminated and have high counts over the entire detector, we can use them to estimate the response of grot-affected pixels. The last study of grot-affected pixels was done in 2003 (Schultz et al, NICMOS ISR 2003-003) as part of the flat-field monitoring of stability in NICMOS.

In a manner similar to that used in 2003, we utilized the post-NCS flat-field observations:

1. A well-sampled (F160W) flat-field, based on 2002-2008 data, is re-inverted¹.
2. The re-inverted flat is smoothed.
3. The smoothed flat is subtracted from the re-inverted flat-field.
4. Grot pixels are defined as pixels deviating more than 4σ in the subtracted image, excluding bad (DQ=32) pixels.

We find that the new data results in fewer grot-affected pixels compared to the existing grot mask made in 2002, as can be seen in Table 3.

¹ This is because NICMOS flat-fields are, by construction, inverted images, where a high pixel value means a low response.

	Existing	New
NIC1	180	170
NIC2	243	123
NIC3	249	113

Table 3: The number of old and new grot-affected pixels in each camera.

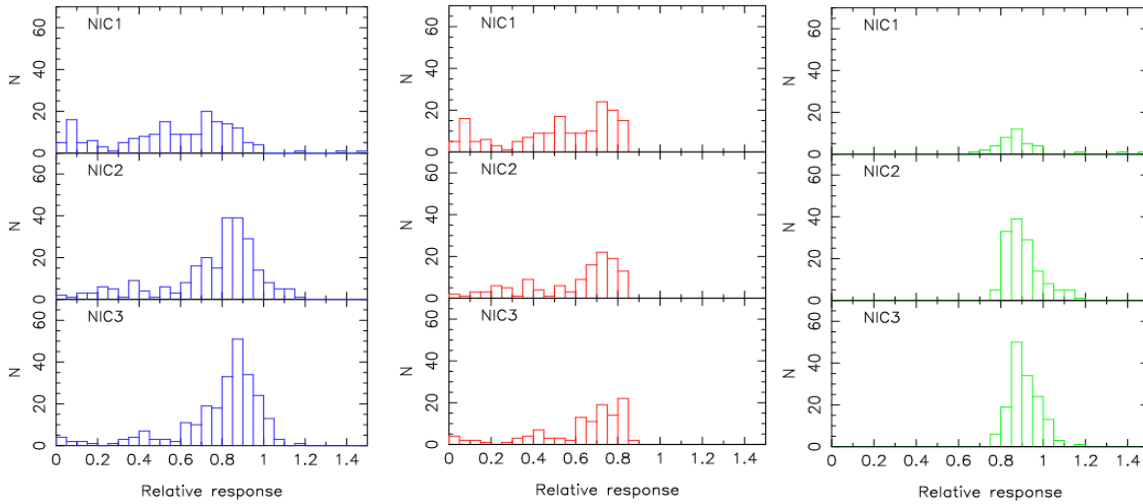


Figure 5: The number of pixels by relative DQE response of pixels, per camera. The left panel (blue) shows the old grot mask. The center panel (red) shows the new selected grot pixels. The right panel (green) shows the “extra” grot pixels found in the old mask, but not in the new mask.

Due to the large difference in the number of old and new grot pixels, it is useful to examine the relative Detector Quantum Efficiency (DQE) response of the pixels that are not being flagged in the new analysis, but were previously flagged. The relative DQE response can be determined by dividing the flat-field image by the smoothed flat-field image. In the resultant ratio image, a “normal” pixel (not grot-affected) has a response equal to unity.

The left panel of Figure 5 shows the relative response of the pixels in the old grot mask, while the middle panel shows the new selection. The analysis of the new data selects grot-affected pixels as those with a response ≤ 0.8 . The pixels that are flagged as grot-affected in the old masks *and not* flagged as grot in the new analysis (“extra” grot) are shown in the right panel of the figure. It is clear that these pixels have close to normal responses (0.8–1.2).

In order to further examine the nature of the “extra” grot pixels and see if we can safely recover these pixels for science observations, we compare the RMS of these pixels to the

RMS of normal non-grot pixels, by camera. The RMS is calculated pixel by pixel from the stack of individual flat-field observations used to create the combined flat-field used here. If, for example, grot has moved between epochs, then it is expected that the RMS would be higher for pixels affected by the moved grot.

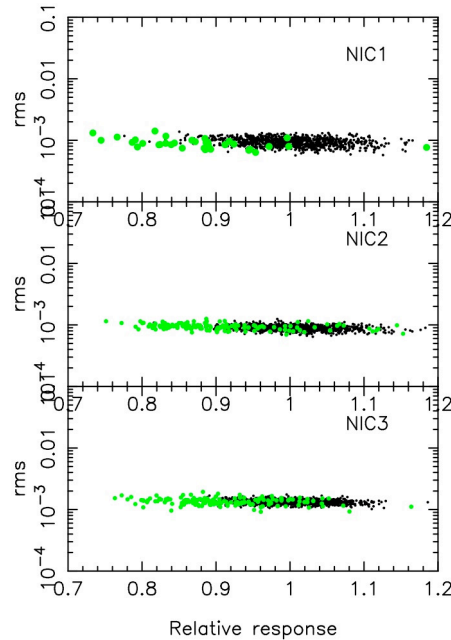


Figure 6: RMS per pixel versus relative DQE response. Small black dots are non-flagged, “normal” pixels and large green dots are “extra” grot pixels.

We see in Figure 6 that the RMS of the “extra” grot pixels (large green dots) are similar to those of non-flagged, “normal” pixels (small black dots). This, along with the fact that the “missing grot” pixels have relative DQE responses in the normal range, provides confidence that these pixels have proper sensitivities for science observations. Therefore, we should be able to recover these pixels for science and set their DQ flags back to zero, or “deflag” them.

We also want to know if there is a significant number of grot pixels that change with time. In Table 4, we list the number of grot-affected pixels in the old grot masks, the new grot masks, during 2002, and during 2008. We see that all three cameras show fewer grot-affected pixels in the new masks, but the numbers are not significantly different between 2002 and 2008. We therefore do not create time-dependent grot masks, but incorporate all data between 2002 and 2008 into single masks, one for each camera.

	Old	New	2002	2008
NIC1	180	170	172	174
NIC2	243	123	119	139
NIC3	249	113	113	112

Table 4: The number of grot-affected pixels with time.

As a final selection of grot-affected pixels, we include all “ 4σ pixels” from the above discussion as grot pixels (*except* those that have a response >0.8 and a normal RMS, which are instead addressed by the flat-fields). This selection somewhat reduces the number of grot pixels compared to that given in Tables 3 and 4. The final number of grot pixels for the three cameras are given in Table 5. These pixels will be marked with DQ=16 in the same mask files as the bad pixels (DQ=32). The difference between the old and new grot masks can be seen clearly in Figure 7 below, with the old masks shown across the top and the new grot masks shown along the bottom. The reduced number of grot pixels is most apparent in NIC3.

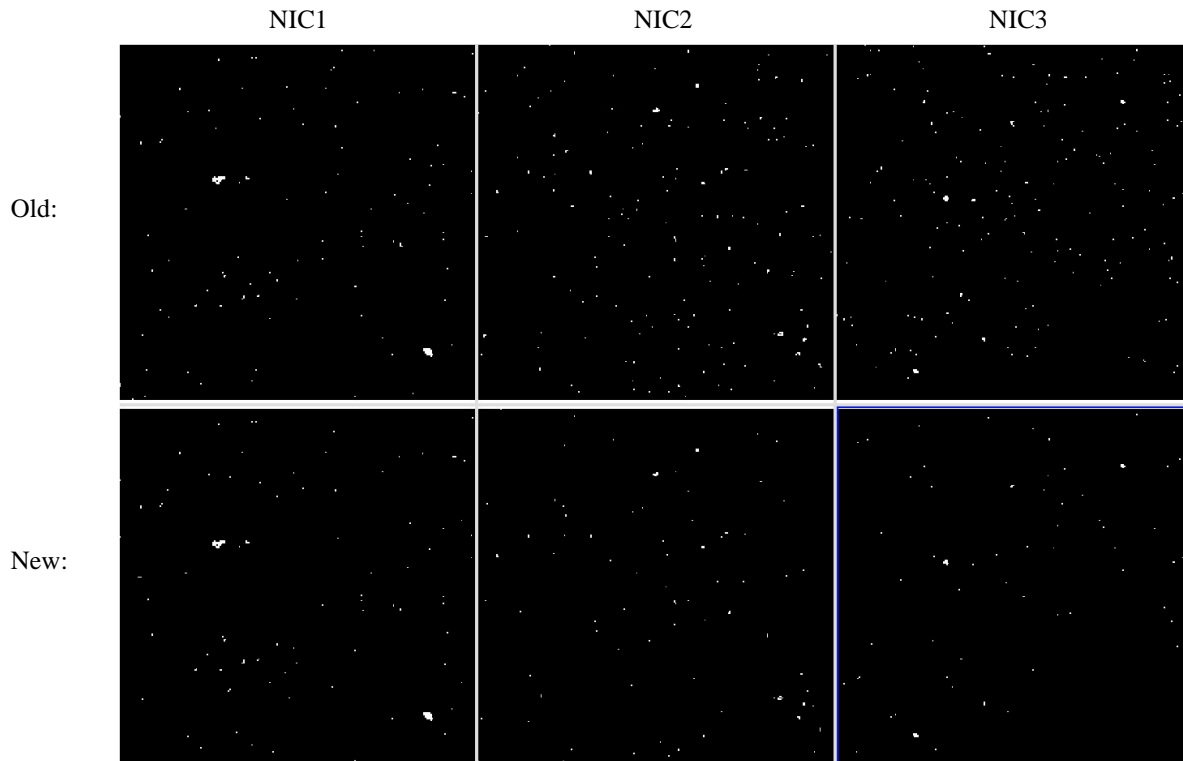


Figure 7: Old and new grot masks for each camera of NICMOS.

New Static DQ Masks for NICMOS

The NICMOS bad pixel masks for each camera were generated by placing the DQ flag values in the DQ extension of the MASKFILE reference files. Table 5 lists the number of pixels for both the old and new masks, with grot and bad pixels distinguished.

	Grot, DQ=16		Bad, DQ=32	
	Old	New	Old	New
NIC 1	180	163	193	281
NIC 2	243	119	656	696
NIC 3	249	96	446	488

Table 5: The final, new static DQ masks for all three NICMOS cameras.

We also present the new final, complete, static DQ masks for each camera in Figure 8 below. We can visually see the reduction in grot-flagged pixels, notably in NIC2, but especially in NIC3.

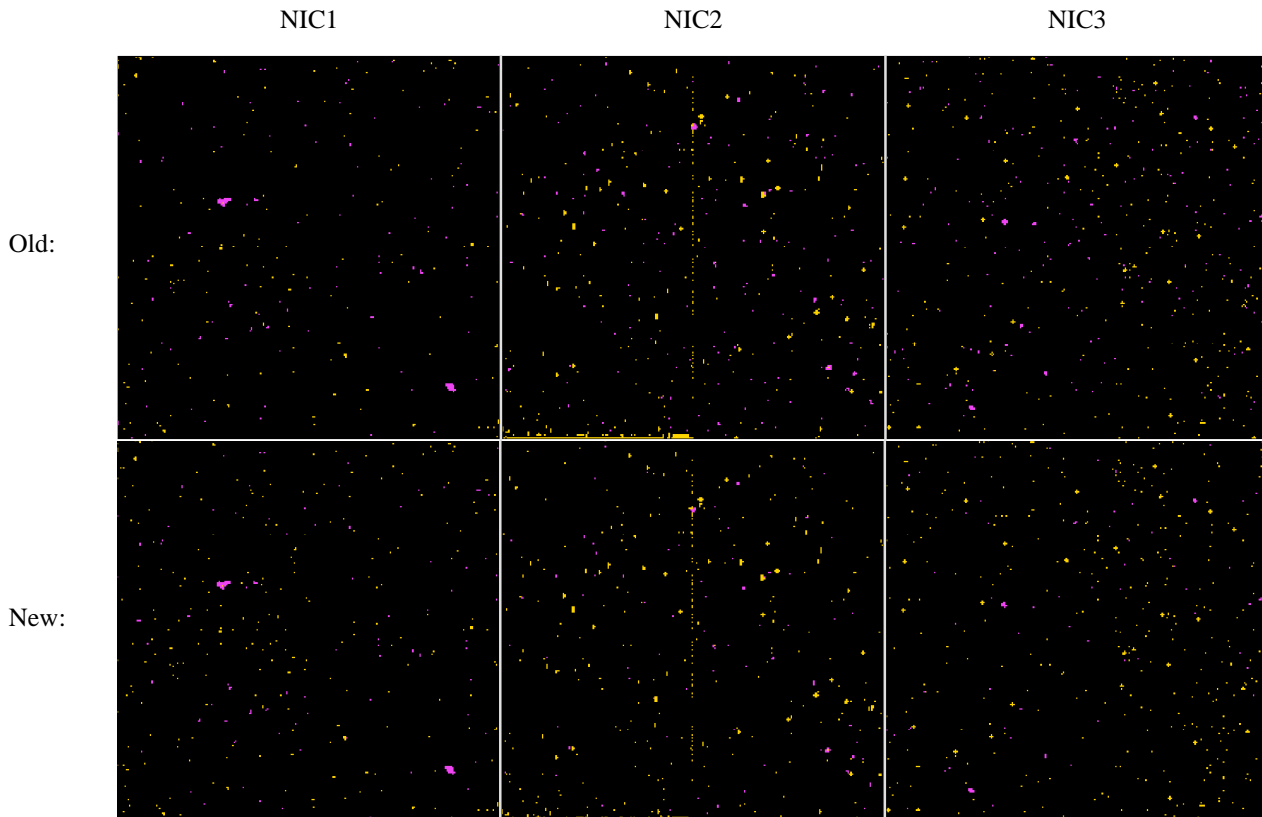


Figure 8: Old and new final DQ masks for each camera. Yellow pixels are bad pixels, purple pixels are grot-affected pixels.

These new mask files have been delivered to CDBS and are available to the pipeline for calibration and to users via the NICMOS Reference Files web page at <http://www.stsci.edu/hst/observatory/cdbs/SIfileInfo/NICMOS/reftablequeryindex>.

Conclusions

We have used NICMOS SPARS64 images to create new “hot+cold” pixel masks and flat-field calibration image to determine current grot-affected pixels, for calibrating NICMOS images. We have shown that there is only a weak temporal dependence of the number of flagged pixels and have therefore created only a single MASKFILE for each camera for the post-NCS era. Compared to the previous mask from 2002, these new masks contain a slightly higher number of bad pixels (DQ=32), while the number of grot pixels (DQ=16) has decreased. As always, well-dithered observations is the recommended way to handle bad pixels of all types and for most types of science.

Acknowledgements

We would like to thank the entire NICMOS team for their assistance and enlightening discussions. We also thank Anton Koekemoer for the proofreading and comments.

References

- Schultz, A. et al. 2003, NICMOS ISR 2003-003
- Sosey, M. and Bergeron, L. E. 1999, NICMOS-ISR-99-008
- Sosey, M. 2002, NICMOS ISR 2002-001